

## Anti-Collagen I/COL1A1 Antibody Picoband®

Catalog Number: PB9939

### About Col1a1

Collagen, type I, alpha 1, also known as COL1A1, is a human gene that encodes the major component of type I collagen, the fibrillar collagen found in most connective tissues, including cartilage. This gene is mapped to 17q21.33. And this gene encodes the [pro-alpha1 chains](#) of type I collagen whose triple helix comprises two alpha1 chains and one alpha2 chain. Type I is a fibril-forming collagen found in most connective tissues and is abundant in bone, cornea, dermis and tendon. Mutations in this gene are associated with osteogenesis imperfecta types I-IV, Ehlers-Danlos syndrome type VIIA, Ehlers-Danlos syndrome Classical type, Caffey Disease and idiopathic osteoporosis.

### Overview

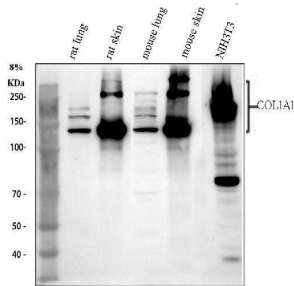
Product Name	Anti-Collagen I/COL1A1 Antibody Picoband®
Reactive Species	Mouse, Rat
Description	Boster Bio Anti-Collagen I/COL1A1 Antibody Picoband® catalog # PB9939. Tested in IHC, WB applications. This antibody reacts with Mouse, Rat. The brand Picoband indicates this is a premium antibody that guarantees superior quality, high affinity, and strong signals with minimal background in Western blot applications. Only our best-performing antibodies are designated as Picoband, ensuring unmatched performance.
Application	IHC, WB
Clonality	Polyclonal
Formulation	Each vial contains 4 mg Trehalose, 0.9 mg NaCl and 0.2mg Na <sub>2</sub> HPO <sub>4</sub> .
Storage Instructions	Store at -20°C for one year from date of receipt. After reconstitution, at 4°C for one month. It can also be aliquotted and stored frozen at -20°C for six months. Avoid repeated freeze-thaw cycles.
Host	Rabbit
Uniprot ID	P11087

### Technical Details

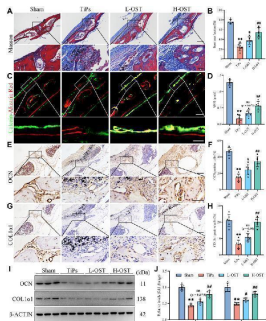
Immunogen	A synthetic peptide corresponding to a sequence at the C-terminus of mouse Collagen I, different from the related human sequence by three amino acids, and identical to the related rat sequence.
Recommended Detection Systems	Boster recommends Enhanced Chemiluminescent Kit with anti-Rabbit IgG (EK1002) for Western blot, and HRP Conjugated anti-Rabbit IgG Super Vision Assay Kit (SV0002-1) for IHC(P).
Cross Reactivity	No cross-reactivity with other proteins
Isotype	Rabbit IgG
Form	Lyophilized

Concentration	Adding 0.2 ml of distilled water will yield a concentration of 500 ug/ml.
Purification	Immunogen affinity purified.
Suggested Dilutions	Western blot, 0.1-0.5ug/ml, Mouse, Rat Immunohistochemistry (Paraffin-embedded Section), 0.5-1ug/ml, Mouse, Rat

## Anti-Collagen I/COL1A1 Antibody Picoband® (PB9939) Images

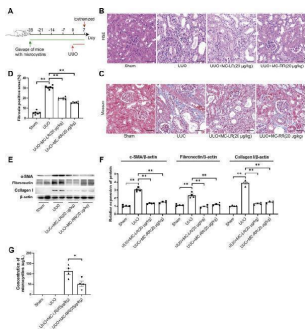


Western blot analysis of COL1A1 using anti-COL1A1 antibody (PB9939). Electrophoresis was performed on a 8% SDS-PAGE gel at 80V (Stacking gel) / 120V (Resolving gel) for 2 hours. The sample well of each lane was loaded with 30 ug of sample under reducing conditions. Lane 1: rat lung tissue lysates, Lane 2: rat skin tissue lysates, Lane 3: mouse lung tissue lysates, Lane 4: mouse skin tissue lysates, Lane 5: mouse NIH/3T3 whole cell lysates. After electrophoresis, proteins were transferred to a nitrocellulose membrane at 150 mA for 50-90 minutes. Blocked the membrane with 5% non-fat milk/TBS for 1.5 hour at RT. The membrane was incubated with rabbit anti-COL1A1 antigen affinity purified polyclonal antibody (PB9939) at 0.5 ug/mL overnight at 4°C, then washed with TBS-0.1%Tween 3 times with 5 minutes each and probed with a goat anti-rabbit IgG-HRP secondary antibody (Catalog # BA1054) at a dilution of 1:5000 for 1.5 hour at RT. The signal is developed using an ECL Plus Western Blotting Substrate (Catalog # AR1196-200) with Tanon 5200 system. A specific band was detected for COL1A1 at approximately 130,180-200 kDa. The expected band size for COL1A1 is at 138 kDa.

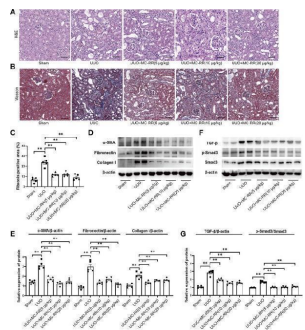


OST treatment attenuated TiPs-induced osteogenesis inhibition in vivo. ( A ) Representative Masson's trichrome staining images of calvarial sections. Scale bar, 200  $\mu$ m (upper), 50  $\mu$ m (lower). ( B ) Quantitative analysis of new bone area fraction (%) determined by Masson's trichrome staining. ( C ) Representative images of calcein (green) and alizarin red (red) double labeling with a 10-day interval. Scale bar, 50  $\mu$ m (upper), 20  $\mu$ m (lower). ( D ) Quantitative analysis of average periosteum mineral apposition rates (MAR,  $\mu$ m/d). ( E-F ) Representative images and quantitative analysis of immunohistochemical (IHC) staining for osteocalcin (OCN). Scale bar, 100  $\mu$ m (upper), 50  $\mu$ m (lower). ( G-H ) Representative images and quantitative analysis of IHC staining for collagen type I alpha 1 (COL1 $\alpha$ 1). Scale bar, 100  $\mu$ m (upper), 50  $\mu$ m (lower). ( I ) Western blot analysis of the expression of osteogenic markers (OCN, COL1 $\alpha$ 1) in calvarial bone tissue samples from each group. n = 6. The selected images reflect typical examples from each group, closely representing the median degree as per statistical analysis. Data are presented as mean  $\pm$  SD. One-way ANOVA with Tukey's post hoc test. The relative COL1 $\alpha$ 1 protein levels were analyzed using Brown-Forsythe and Welch ANOVA tests followed by Tamhane T2 post hoc tests. \*\* P

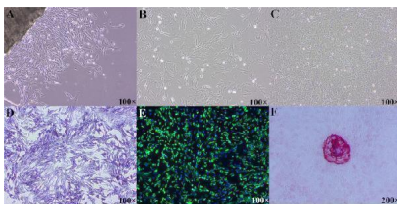
Antifibrotic effect of microcystin (MC) in renal fibrosis mice. Mice were treated with MC-LR (20 ug/kg/day) or MC-RR (20 ug/kg/day) by intragastrical administration for 4 weeks in advance, and then unilateral ureteral ligation was performed to construct a mouse model of obstructive renal fibrosis. The operated mice were administrated with MC-LR



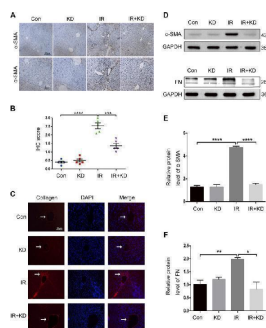
or MC-RR for another week, and then were euthanized for further analysis. (A) Schematic diagram of the experimental design. Forty mice were divided into four groups, Sham, unilateral ureteral obstruction (UUO), UUO + MC-LR, and UUO + MC-RR groups, each with 10 mice. No mice died during the experiment. (B,C) Kidney tissue sections were employed for H&E and Masson staining (scale bar: 40  $\mu$ m). (D) Fibrosis positive area in Masson staining were assessed by pathologist blind to this study (n = 6). (E,F) The protein level of  $\alpha$ -smooth muscle actin ( $\alpha$ -SMA), fibronectin and collagen I were measured in the obstructive renal tissues of UUO mice by western blot. \* p < 0.05, \*\* p < 0.01 determined by one-way ANOVA with S-N-K post hoc analysis. (G) Residual contents of MC were detected in the kidney tissues of model mice treatment with MC-LR or MC-RR using the ELISA method. Data were analyzed using independent Student's t-test, \* p < 0.05. Index in PubMed under a CC BY license. PMID: 35754468



Renoprotection effect of microcystin (MC)-RR in different doses on unilateral ureteral obstruction (UUO) mice. The regimen of MC-RR was used in UUO mice. Twenty-five mice were divided into five groups, Sham, UUO, and UUO mice with treatment of MC-RR in three different doses (5, 10, and 20  $\mu$ g/kg/day), each group with 5 mice. (A,B) Kidney tissue sections were employed for H&E and Masson staining (scale bar: 40  $\mu$ m). (C) Fibrosis positive area in Masson staining were assessed by pathologist blind to this study (n = 5). (D,E) Protein level of  $\alpha$ -smooth muscle actin ( $\alpha$ -SMA), fibronectin, and collagen I were measured in the renal tissues of UUO mice by western blot. (F,G) Protein expression of TGF- $\beta$ , p-Smad3, and Smad3 in kidney tissue was measured by western blot. \* p < 0.05, \*\* p < 0.01 determined by one-way ANOVA with S-N-K post hoc analysis. Index in PubMed under a CC BY license. PMID: 35754468

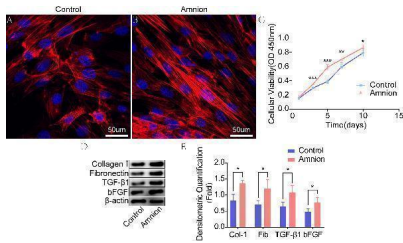


Morphological features and identification of primary cultured tibial osteoblasts of broiler chicks. (A) Morphological image of P0 cells, day of 3 culture; (B) morphological image of P1 cells, day of 2 culture; (C) morphological image of P1 cells, day of 10 culture; (D) primary osteoblasts were positive in ALP staining; (E) immunofluorescence of COL1A1 in the primary tibial osteoblasts; (F) mineralized nodules were positive in ARS staining. ALP, alkaline phosphatase; COL1A1, collagen type I alpha 1; ARS, alizarin res S. Index in PubMed under a CC BY license. PMID: 35392115

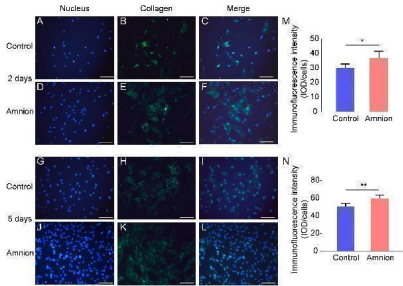


KD inhibits the expression of the fibrosis-related proteins in the rat model (A) The results of the IHC staining displayed the expression of  $\alpha$ -SMA of the liver histology slices. KD significantly reduced the expression of brown stained  $\alpha$ -SMA after irradiation (B) The IHC scores for grading the expression of  $\alpha$ -SMA (C) Expression and localization of collagen in the liver tissue. The red stain represented collagen, which indicated that collagen expression in the IR + KD group was significantly lower than that in the IR group

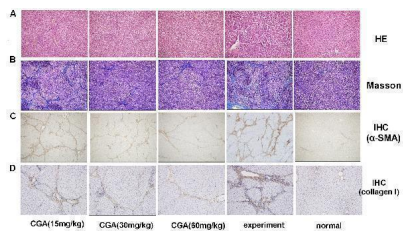
(D-F) The results of the western blots showed the expression of alpha -SMA and FN proteins in the liver tissue. The administration of KD after irradiation resulted in decreased expression of a -SMA and FN. For all results in this figure, original magnification,  $\times 100$  and  $\times 200$ . Mean  $\pm$  SEM. n. s. denotes not significant; \*  $p < 0.05$ , \*\*  $p < 0.01$ , \*\*\*  $p < 0.001$ , \*\*\*\*  $p < 0.0001$ . Index in PubMed under a CC BY license. PMID: 35126163



Fluorescence images of tenocytes after 5 days of culture on the surface of a culture plate (control group) and acellular amniotic membrane (amniotic group). Tenocytes presented a clear cytoskeleton, good biocompatibility with acellular amniotic membrane, and even distribution on the surface of the materials, showing better growth activity than the control group (A,B) . Cell viability was measured by CCK-8, and the proliferation curve of tenocytes in the control and amniotic membrane groups was drawn (C) . Western blot assay for collagen I, fibronectin, TGF-beta1, and bFGF expression in the tenocytes of the control and amniotic groups for 1 week (D,E) . \*  $p < 0.05$ ; \*\*  $p < 0.01$ ; and \*\*\*  $p < 0.001$ . Index in PubMed under a CC BY license. PMID: 32478059

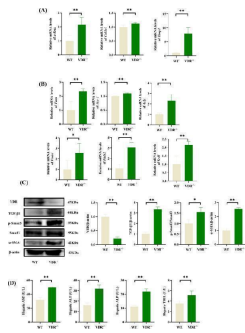


Representative immunofluorescence images of collagen I. Fluorescent micrographs of tenocytes after 2 and 5 days of culture on the surface of a culture plate and acellular amniotic membrane. Tenocyte nucleus shape observed under a fluorescence microscope (A,D,G,J) . Collagen I presented positive after the fluorescent FITC mark was observed under a fluorescence microscope (B,E,H,K) . Tenocyte nucleus and collagen I merging (C,F,I,L) . The corresponding semi quantitative analysis of collagen fluorescence intensity in panels (M,N) (scale bar = 50 μm, n = 5, \*  $P < 0.05$  and \*\*  $P < 0.01$ ). Index in PubMed under a CC BY license. PMID: 32478059

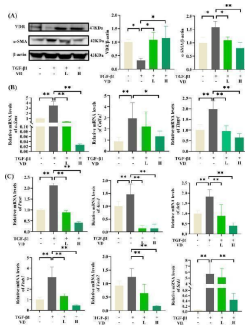


Evaluation of the effect of CGA on liver histopathological and immunohistochemistry (IHC) in liver tissue. (A) Histological images of rat livers stained with H&E (original magnification,  $\times 200$ ). (B) The histopathologic detection of collagen in the liver by Masson's trichrome stain (original magnification,  $\times 100$ ). (C,D) Effects of CGA on alpha-SMA and collagen I expression were examined with immunohistochemistry in liver tissue (original magnification,  $\times 100$ ). Index in PubMed under a CC BY license. PMID: 29311932

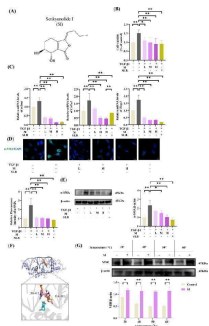
VDR deficiency exacerbated hepatic fibrosis and steatosis in mice. A mRNA levels of fibrogenic markers ( alpha-Sma , Coll1a1 , and Timp1 ). B mRNA levels of lipogenic enzymes ( Fasn , Acc-1 , and Acly ) and fatty acid desaturases ( Fads1/2 and Scd1 ) ( n = 5). C Western blot analysis of VDR and TGFbeta/Smad pathway ( n = 3), D Serum levels of liver function markers (AST, ALT, ALP, and TBIL) ( n = 5). \*  $P < 0.05$ , \*\*  $P < 0.01$  Full size image Index in PubMed under a CC BY license. PMID: 40514735



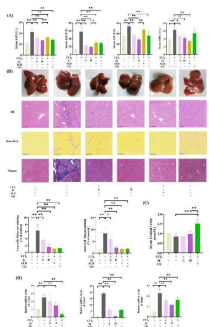
VDR activation attenuated TGF-beta1-induced fibrosteatotic changes in HSCs. A Western blot analysis of VDR and alpha-SMA (n = 3). B mRNA levels of fibrogenic markers ( alpha-Sma , Col1a1 , and Timp1 ). C mRNA levels of lipogenic enzymes ( Fasn , Acc-1 , and Acly ) and fatty acid desaturases ( Fads1/2 and Scd1 ) (n = 6). \* P < 0.05, \*\* P < 0.01 Full size imageIndex in PubMed under a CC BY license. PMID: 40514735



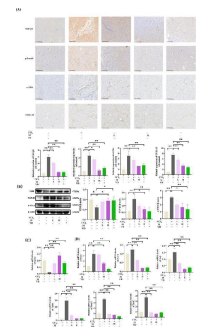
SI inhibited TGF-beta1-induced activation of HSCs. A Chemical structure of the SI. B Cell viability of HSCs. C mRNA levels of fibrogenic markers ( alpha-Sma , Col1a1 , and Timp1 ). D Immunofluorescence analysis of alpha-SMA. scale bar = 20 um. (n = 6). E Western blot analysis of alpha-SMA. F Molecular docking results of VDR and SI. G CETSA analysis. (n = 3) \* P < 0.05, \*\* P < 0.01 Full size imageIndex in PubMed under a CC BY license. PMID: 40514735

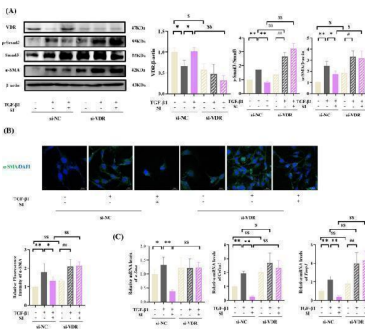


SI ameliorated CCl4-induced liver fibrosis in mice. A Serum levels of liver function markers (AST, ALT, ALP, and TBIL). B Liver tissue photograph and histopathological analysis (HE, Sirius Red, Masson), scale bar = 200 um. C Serum calcium concentrations. D mRNA levels of fibrogenic markers ( alpha-Sma , Col1a1 , and Timp1 ). (n = 5) \* P < 0.05, \*\* P < 0.01 Full size imageIndex in PubMed under a CC BY license. PMID: 40514735

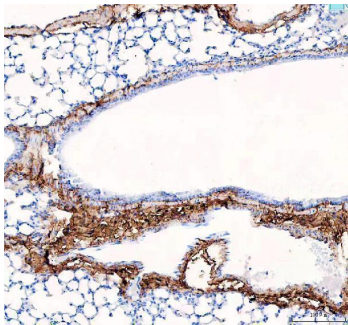


SI regulated VDR and fatty acid metabolism to suppress TGFbeta/Smad pathway in CCl4-induced mice. A Immunohistochemistry analysis of TGF-beta1, p-Smad3, alpha-SMA, COL1 A1. scale bar = 200 um. (n = 5). B Western blot analysis of VDR, TGF-beta1, and alpha-SMA. C mRNA levels of Cpt1a. D mRNA levels of lipogenic enzymes ( Fasn , Acc-1 , and Acly ) and fatty acid desaturases ( Fads1/2 and Scd1 ) (n = 6) \* P < 0.05, \*\* P < 0.01 Full size imageIndex in PubMed under a CC BY license. PMID: 40514735

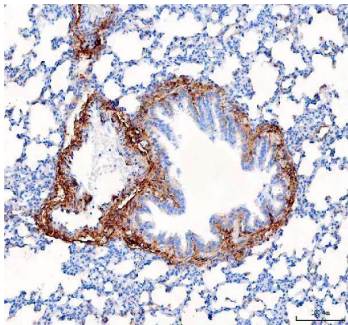




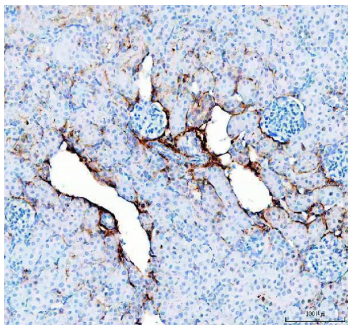
VDR knockout abolished the SI-induced inhibition of HSCs activation. A Western blot analysis (n = 3). B Immunofluorescence analysis of alpha-SMA. scale bar = 20 um. (n = 6). C mRNA levels of fibrogenic markers ( alpha-Sma , Col1a1 , and Timp1 ). (n = 6) \*P < 0.05, \*\*P < 0.01 compared with si-NC + TGF-beta1; \$ P < 0.05, \$\$ P < 0.01 compared with si-NC; # P < 0.05, ## P < 0.01 compared with si-VDR + TGF-beta1 Full size imageIndex in PubMed under a CC BY license. PMID: 40514735



IHC analysis of COL1A1 using anti COL1A1 antibody (PB9939). COL1A1 was detected in a paraffin-embedded section of mouse lung tissue. Heat mediated antigen retrieval was performed in EDTA buffer (pH 8.0, epitope retrieval solution). The tissue section was blocked with 10% goat serum. The tissue section was then incubated with 2 ug/ml rabbit anti-COL1A1 Antibody (PB9939) overnight at 4°C. Peroxidase Conjugated Goat Anti-rabbit IgG was used as secondary antibody and incubated for 30 minutes at 37°C. The tissue section was developed using HRP Conjugated Rabbit IgG Super Vision Assay Kit (Catalog # SV0002) with DAB as the chromogen.



IHC analysis of COL1A1 using anti COL1A1 antibody (PB9939). COL1A1 was detected in a paraffin-embedded section of rat lung tissue. Heat mediated antigen retrieval was performed in EDTA buffer (pH 8.0, epitope retrieval solution). The tissue section was blocked with 10% goat serum. The tissue section was then incubated with 2 ug/ml rabbit anti-COL1A1 Antibody (PB9939) overnight at 4°C. Peroxidase Conjugated Goat Anti-rabbit IgG was used as secondary antibody and incubated for 30 minutes at 37°C. The tissue section was developed using HRP Conjugated Rabbit IgG Super Vision Assay Kit (Catalog # SV0002) with DAB as the chromogen.



IHC analysis of COL1A1 using anti COL1A1 antibody (PB9939). COL1A1 was detected in a paraffin-embedded section of rat kidney tissue. Heat mediated antigen retrieval was performed in EDTA buffer (pH 8.0, epitope retrieval solution). The tissue section was blocked with 10% goat serum. The tissue section was then incubated with 2 ug/ml rabbit anti-COL1A1 Antibody (PB9939) overnight at 4°C. Peroxidase Conjugated Goat Anti-rabbit IgG was used as secondary antibody and incubated for 30 minutes at 37°C. The tissue section was developed using HRP Conjugated Rabbit IgG Super Vision Assay Kit (Catalog # SV0002) with DAB as the chromogen.

## 59 Publications Citing This Product

1. PubMed ID: 10.1038/s41598-020-67514-4, Investigating the antifibrotic effect of the antiparasitic drug Praziquantel in in vitro and in vivo preclinical models

2. PubMed ID: 30888602, Wei X, Bao Y, Zhan X, Zhang L, Hao G, Zhou J, Chen Q. MiR-200a ameliorates peritoneal fibrosis and functional deterioration in a rat model of peritoneal dialysis. *Int Urol Nephrol*. 2019 May; 51(5):889-896. doi:10.1007/s11255-019-02122-4. Epub 2019 Mar 19. PMID:30888602; PMCID:PMC6499761.

3. PubMed ID: 31169440, Li X, Bu X, Yan F, Wang F, Wei D, Yuan J, Zheng W, Su J, Yuan J. Deletion of discoidin domain receptor 2 attenuates renal interstitial fibrosis in a murine unilateral ureteral obstruction model. *Ren Fail*. 2019 Nov; 41(1):481-488. doi:10.1080/0886022X.2019.1621759. PMID:31169440; PMCID:PMC6567249.

Visit [bosterbio.com/anti-collagen-i-picoband-trade-antibody-pb9939-boster.html](https://bosterbio.com/anti-collagen-i-picoband-trade-antibody-pb9939-boster.html) to see all 59 publications.

## Submit a product review to Biocompare.com

Submit a review of this product to Biocompare.com to receive a \$20 Amazon.com giftcard! Your reviews help your fellow scientists make the right decisions. Thank you for your contribution.



Anti-Collagen I/COL1A1 Antibody

For Research Use Only. Not for use in diagnostic procedures.